The Potential for Solar Electricity Generation in San Francisco

A Report to the Environmental Law and Justice Clinic of
Golden Gate University Law School

Karina Garbesi, Ph.D. and Emily Bartholomew

June 1, 2001

Summary of findings

- Our estimates of annual PV output potential range from 550 to 1300 GWh per year. At the high end, this is comparable to current residential (and industrial) electricity use in San Francisco. (1 GWh = one million kilowatt-hours).
- Our low estimates for total PV electricity output potential during peak times in late October (when potential is not at its highest) range from 240 MW to 600 MW, bounding the size of the proposed Potrero Unit 7, at 540 MW (1 MW = one million watts). Clearly, rooftop photovoltaic systems in San Francisco could provide significant power output compared to the proposed Unit 7 at Potrero, greatly reducing, or potentially eliminating, the need for the new unit, particularly if PV implementation is combined with efficiency measures that reduce demand.
- Over the 30-year period for which solar data are available for San Francisco, the standard deviation of the annual average solar radiation was less than 2.5% of its average value. Thus, the solar resource can be relied upon as a stable source of power, and to deliver that power when needed at times of peak electricity demand.
- Because the demand for new power is driven by growing peak use, PV system output, which effectively shaves the demand for conventional power during peak times, is very valuable. Thus rooftop PV systems could greatly reduce the amount of centralized, in-area generation needed to meet the power reliability requirements established by the ISO and the City of San Francisco.
- Rooftop PV systems would have *no* requirements for new land. Nor do they foul the air. These systems are commercially available, function well in the Bay Area, and are being installed in some places at costs comparable to those paid by the State of California for new gas-fired power capacity. The State of California currently offers a $4.5/W rebate on installed PV systems. (Emerging Renewables Buydown Program www.energy.ca.gov).
- PV systems offer substantial ancillary cost savings relative to centrally produced power that greatly enhance their real value with respect to centralized power generation. Rooftop PV systems limit the necessity for costly distribution system upgrades because they generate power where it is needed, rather than having to transmit it to the point of use. As distribution costs about as much as generation per delivered kWh, this effectively doubles that real value of PV system investments. Using large numbers of small-scale generators, such as PV, also greatly reduces the need for costly reserve power capacity needed to maintain power reliability in the City during times when large local units are being serviced. The equivalent in PV systems terms to Unit 7 shutting down would be to have 135,000 4-kW PV rooftop systems fail simultaneously — an utterly improbable prospect. This again represents large potential savings. If one can reduce reserve capacity, lets say, by 75%, this could eliminate the need to rely on the dirtiest oldest plants during periods when the primary capacity is down. Thus one is likely to avoid peak pollution problems.

Contents

Background

Photovoltaic Electricity Generation

Generating electricity from sunlight using photovoltaic (PV) panels is a logical way to reduce peak demand. Even in San Francisco, peak electricity demand occurs on the hottest days of the year during the hottest time of the day (usually early afternoon), driven primarily by commercial air conditioning (AC) loads. When the fog comes in, demand abates. In San Francisco, peak demand days occur during summer and early fall (CAISO et al. 2000). This paper makes an estimate of the total PV generation potential in San Francisco — both in terms of peak output and total annual generation.

PV system output is proportional to the amount of solar radiation received. It is therefore highest under clear-sky conditions in summertime. Those are the same conditions that produce the hottest days with the highest AC demand. Under clear sky conditions, maximum solar intensity occurs at solar noon (the instant that the sun is highest in the sky[1]. Peak demand usually occurs in mid afternoon. But PV system output depends on the orientation of the panels. Panels oriented west of south produce peaks outputs after solar noon. Whereas those oriented east produce peak outputs earlier. Similarly the amount of electricity generated during different seasons can be varied by adjusting the tilt angle of the solar collector (see Figure 1 for definition of tilt angle). Assuming a site does not have systematic differences in morning vs. afternoon cloud cover, the maximum annual output is achieved by facing panels due south with a tilt angle equal to the latitude angle (~37.5^{o}). The typical practice in the solar industry now, however, is to simply place PV panels flush with the southerly facing roof, using panel area, rather than orientation to generate the desired output. This is both for aesthetic and cost reasons. On flat rooftops typical of commercial buildings one can either use banks of tilted panels, separated to avoid shading each other. Or, one can simply cover the roof with horizontal panels. The largest system installed it the Unites States (a 500 kW system on Santa Rita Jail in California, designed and installed by Powerlight of Berkeley) is designed this way. It uses insulated models that plug together yielding ancillary cost savings through HVAC cost reductions (from enhanced roof insulation) and longer roof life.

[1] Solar noon differs from local time noon because time zones create abrupt discontinuities in clock times. That is, solar noon arrives later as one moves west through a time zone. But, clock time does not. Daylight savings also changes clock times relative to solar times. None of these issues affect solar output, however, because PV panels do not know how to tell time.

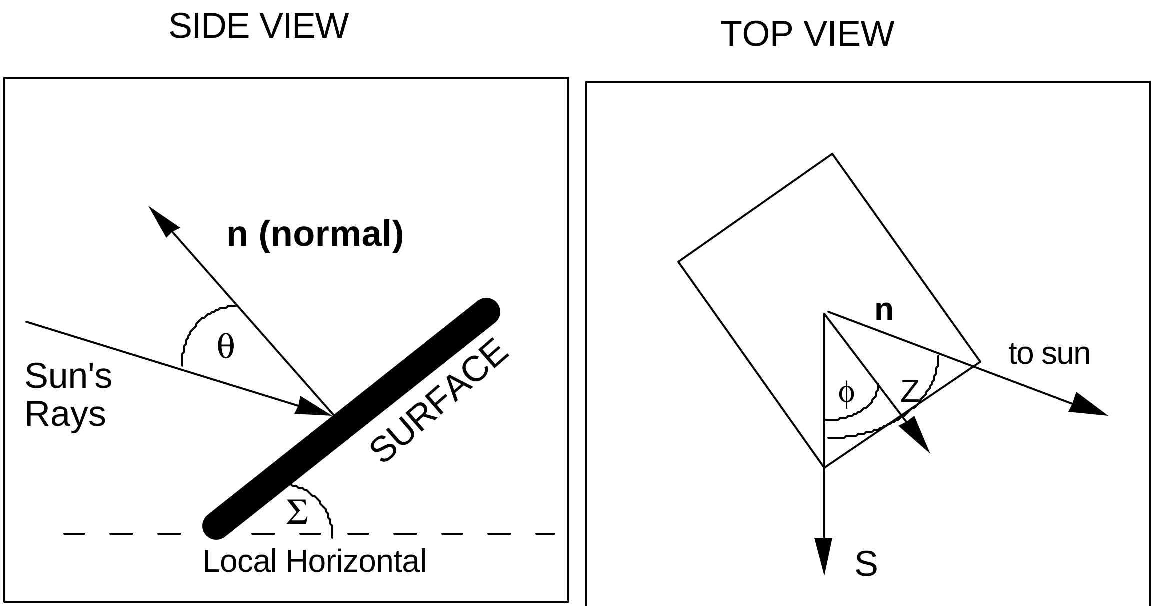

Figure 1. The figures show various angles used in describing the orientation of solar panels. Of interest here, the tilt angle, shown in the left figure, is the angle between the horizontal and the panel's surface.

Cost of PV vs. New Gas-fired Power Plant Capacities in California
Appendix A documents the prices for new gas-fired power plant capacity in contracts and memoranda of understanding recently signed by Governor Davis. These range from \$4.6/W and \$6.3/W. According to the Sacramento Municipal Utility District website (http://www.newrules.org/electricity/smud.html), SMUD is now installing PV systems for \$4.25/W. While it is true that lower PV system capacity factors (~0.25) increase their per kWh cost of energy relative to gas-fired plants, the capacity cost (\$/W) may be more relevant than the energy cost for plants contracted to meet peak demand.[2] Or in other words, peaking plants have their capacity factors reduced anyway because they are not needed much of the time. In effect this helps even out the prices of PV and gas-fired power.

PV offers additional cost advantages that are typically ignored, some of which directly affect the retail price of power. In terms of power reliability, it is far less likely to simultaneously loose 540 MW of power from a very large number of small generating systems than from one large system. This implies that far less reserve generation is needed to preserve reliability. (In other words, once doesn't need 540 MW of reserve to back up 540 MW of small-scale distributed generation, but one does need it to back up a single critical 540 MW unit). This translates into real overall cost savings in terms of capital expenses on idle plants.

In addition, with PV systems distributed throughout the load area, smaller investments will be needed to increase the capacity of the local distribution system in San Francisco. This contrasts with the addition of 540 MW at Potrero, located south of the main load, for which almost all power must be distributed over substantial distances to the load. In addition to such relatively easily quantified cost benefits are those less easily quantified: in particular reduced health costs

[2] Capacity factors measure actual output with respect to potential peak output averaged over time. PV system capacity factors are about 0.25 because they do not generate power at night. Capacity factors of fuel-driven plants are much higher because they are typically available for generation on demand.

associated with air pollution emissions and the environmental justice implications of who bears those costs. This argument is particularly important for PM10 emissions in the Southeast, which is already out of compliance for PM10 and will have its concentrations driven up by the addition of Unit 7, even if Hunter's Point is shut down (Dames and Moore 2000).

Scope of Paper

This paper estimates the total potential for rooftop PV generation in the City of San Francisco. Such an estimate does not yield the total possible output. For example, a current PV application uses PV panels in parking lots to generate electricity and shade cars simultaneously. Other application currently entering the market uses PV for building facades and even in windows. On the other hand, the California net-metering law currently provides a disincentive for commercial and residential customers to generate more than they use on an annual basis. (Energy generated in excess of annual use is 'donated' to the grid. That is, the system owner received no compensation for it.) However, changes have recently been made that greatly liberalized the net-metering law. Specifically, in April of this year the maximum allowable system size was increased from 10 kW to one MW. Thus, it is not impossible to imagine that the law might ultimately accommodate sale of excess power generation at time of day prices, which could greatly stimulate investment in PV systems.

Methods

This paper estimates PV system output assuming that the PV panels are oriented horizontally. As indicated above, this approach is now used on flat commercial rooftops. On the other hand, it underestimates potential residential output, in which panels are typically placed on southerly-facing, sloped roofs. This orientation yields higher output per unit of panel area. Thus this assumption produces a conservative estimate of potential output, consistent with all other assumptions made in this analysis.

To accommodate different micrometeorological characteristics in different parts of the City we divided the City into the four regions described in Table 1. PV potentials were calculated for the regions individually. This also facilitated greater insight into regional differences in the potential for solar power generation.

Table 1. The City was broken into the following four regions to accommodate different meteorological, topographic, and development characteristics.
.

Region	Neighborhoods included[a]	Map cells included[b]
1 'Western'	Sea Cliff, Presidio Heights, Richmond, Sunset, Golden Gate Heights, Parkside, Pine Lake Park, Merced Manor, West Portal, St. Francis Wood, Balboa Terrace	H – M 6 – 13 and N 6 – 9
2 'Financial'	Marina, Cow Hollow, Russian Hill, North Waterfront, Telegraph Hill, North Beach, Pacific Heights, NobHilll, Chinatown, Financial District, Laurel Heights, Anza Vista Alamo Square, South of Market, South Beach, Height-Ahbury, Hayes Valley, Mission Bay	P 5 – 8 Q – V 3 – 8 W 5 – 8
3 'Southeast'	Mission Dolores, Eureka Valley / Dolores Heights, Mission District Potrero, Noe Valley, Bernal Heights, Glen Park, Silver Terrace, Excelsior, Portola, Bayview, Hunters Point, Bayview Heights, Visitation Valley	R – X 9 – 16 Y 12 – 16 Z 14 – 16
4 'Hills'	Ashbury Heights, Corona Heights, Clarendon Heights, Forest Knolls Twin Peaks, Midtown Terrace, Forest Hill, Miraloma Park, Deamond Heights, Sherwookd Forest, Monterey Heights, Westwood Highlands, Mount Davidson Manor, Westwood Park Sunnyside, Lakeside, Mission Terrace, Ingleside Terrace, Merced Heights, Ingleside, Ingleside Heights, Oceanview, Outer Mission, Crocker Amazon	K – Q 14 – 16 N – O 10 – 13 P – Q 9

[a] Note that neighborhoods that are bisected by quadrant boundaries are not listed by are equally likely to be sampled in that random sampling procedure.
[b] Regions were based on map cells on the Rand McNally, San Francisco and Northern Peninsula City Map, Map by Thomas Brothers Maps. Non-land areas and the parks mentioned in the text were eliminated from these sampling areas. H – M 6 – 13 indicates the inclusion of all cells H6 – H13, J6 – J 13, K6 – K13, etc. Note that the cell letter 'I' is omitted from the map.

The following equation was used to estimate the PV power output:

(1) $$P = R_{sol}\ SF\ RA\ AF\ \varepsilon_{PV}.$$

The parameters are defined in Table 2. This equation was used to calculate the average annual electricity output by setting R_{sol} to the average solar radiation received on a horizontal surface over a one-year period (kWh/m^2/day). It was used to estimate the instantaneous peak power output by setting R_{sol} to the daytime peak power as seen by the horizontal surface (W/m^2).

Table 2. Parameters used in the PV output calculations

Model parameter	Definition	Units
P	the electric power output	
R_{sol}	the solar radiation received per unit horizontal area	kWh/m^2/year (to calculate annual electricity production) W/m^2 (to calculate peak output)
SF	the solar factor, (the fraction of San Francisco Airport solar radiation received in the region of interest)	Unitless
RA	the total roof area of a region	m^2
AF	the accessibility factor, indicates what fraction of rooftops are solar accessible and therefore good locations for PV systems	unitless
ε_{PV}	the efficiency with which PV panels convert sunlight to electricity	unitless

Table 3 documents model input parameters that differ by region. These are discussed in more detail below. The parameters that are independent of region include the solar radiation (R_{sol}), because the solar factor accounts for regional differences, and the PV system efficiency (ε_{PV}). For consistency, the input values used in the model (i.e., in Equation 1) are tabulated in Table 4.

Table 3. Model input parameters that vary by region.

Region	Percent Building Area (Avg)	Area of Region Sampled[a]	Roof Area in region (mi^2)	Roof Area, RA (m^2)	AF min	AF max	Solar Factor (SF)
1 Western	34%	8.75	2.98	7.7052E+06	0.15	0.30	0.7
2 Financial	45%	9.88	4.44	1.1509E+07	0.05	0.20	0.8
3 Southeast	31%	13.88	4.30	1.1140E+07	0.15	0.30	1.0
4 Hills	30%	7.58	2.27	5.8857E+06	0.05	0.20	0.8
Average	35%						
TOTALS		40.08	13.99	3.6240E+07			

[a] The regions exclude major parks and water bodies (see Appendix B for details)

The total roof area of each region was estimated using a CD-ROM-based micro-scale map of the City (San Francisco MicroMap by Zenrin). The map shows individual building footprints of the entire City. The average percentage of land area covered by buildings was estimated using a random sampling procedure described in the Appendix B. The results of the estimates of the percentage of land covered by buildings are shown in Table 3.

Table 4. Model parameters that are independent of region

Parameter	Value	Comments
R_{sol}	4.72 kWh/m^2/day	The average total radiation received over the 30-year period (see Appendix C). R_{sol} was treated as a variable in peak demand calculations.
ε_{PV}	0.10	This is a typical value given in the literature for module efficiency of single crystal panels. It is also the efficiency measured by one of the authors (Garbesi) on her single-crystal rooftop PV system operating in Kensington, California, immediately across the Bay from San Francisco.

The parameter with the largest uncertainty was the roof accessibility factor (how much of total roof area is solar accessible and appropriately oriented for solar energy generation). For buildings with sloped roofs, this means that there must be a solar accessible, southerly-facing roof. We used conservative lower-bound values ranging between 5% and 15%, depending on region, and a range of upper bound estimates that also appears plausible, between 20% and 30%, again varying by region. Areas with higher building density, taller buildings, and more complex topography were assigned lower accessibility factors. These assumptions are summarized in Table 3.

The solar radiation input for the estimates of annual electricity production were based on meteorological data recorded over a 30-year period (1961 – 1990) at the San Francisco Airport. Summary statistics for the 30-year period are given in Appendix C. The data demonstrate that, despite highly dynamic weather conditions in San Francisco, in statistical terms, on an annual basis, solar radiation is very stable. Average solar radiation in San Francisco was 4.72 kWh/m^2/day over the 30 year period. Over the 30-year period, the standard deviation of the average solar radiation was less than 2.5% of its average value. Thus, the solar resource can be relied upon as a stable source of power, and to deliver that power when needed at times of peak electricity demand.

As microclimate varies significantly over the City, and because we did not want to over-estimate PV potential, we thought it desirable to attempt to account for this variability in our analysis. Since the only historical data of solar radiation that we could identify for the Peninsula come from the San Francisco airport, we could not used measured values to make adjustments. We therefore used our judgement as long-term residents and meteorological observers in the region. At times, fog incident upon the western side of the City is blocked from the eastern side by the hills that constitute the central north-to-south portion of the City. In addition, fog passing through the Golden Gate into the Bay, can pass over the northern end of the Peninsula, leaving the southeastern part of the City sunny. To account for this, we assigned *solar factors* to adjust for presumed reductions in solar radiation from the San Francisco Airport, which lies south of the City proper. These factors are also listed in Table 3.

To calculate the peak generation potential of PV systems in San Francisco, we wanted hourly values of solar radiation during clear sky conditions at different times of year. To obtain this we programmed a standard mathematical solar radiation model (Ametek 1984) into a computer spread sheet program. We ran the program for San Francisco's latitude, calculating radiation (direct plus diffuse) incident on a horizontal surface. The model accounts for seasonal changes in atmospheric conditionals that alter solar radiation at the surface. The model results are consistent with the 30-year data set used for the annual estimates of PV output, but easier to use for this purpose. Once the model was run to calculate typical clear-day conditions in summer and fall, Equation 1 was used to calculate diurnal power output given the input parameters listed in Table

3, neglecting the solar factor. The solar factor was not needed, because on those hottest peak-demand days, it is assumed that the entire Peninsula is experiencing clear-sky conditions (at least up until the time that peak use subsides).

Results

Table 5 summarizes the results of our range of estimates of PV output potential in the four regions and in the City as a whole. Not surprisingly the Southeast appears to have the largest potential for PV electricity generation. This is primary because it is the largest area with the largest total roof area. But higher insolation also contributes. The total potential for PV electricity output in SF is estimated to range from about 550 GWh/y to about 1300 GWh/y. The high end of this range is equivalent to total residential (and industrial) use in San Francisco.

Table 5. Minimum and maximum estimates of total annual PV generation potential in San Francisco.

Region	GWh/yr Minimum estimate	GWh/yr Maximum estimate
1 ‘Western’	139	279
2 ‘Financial’	79	317
3 ‘Southeast’	288	576
4 ‘Hills’	41	162
San Francisco total	547	1334

Tables 6a and 6b present potential, diurnal PV system output from San Francisco rooftops during clear sky conditions during the period from June to October. Peak output occurs at solar noon, when the sun is highest in the sky, direct beam radiation is strongest, and the sun’s rays are incident most nearly perpendicular to our assumed-horizontal panels. Our minimum estimates of peak output range from 240 MW in October to 360 MW in June. Our maximum minimum estimates range from 600 MW in October to 900 MW in June. Note that insolation remains fairly high through about 14 hours solar time, before it begins to diminish fairly rapidly.

Table 6a. Minimum estimate of PV power generation potential on San Francisco Rooftops during clear sky conditions calculated for the 21st of June, July, August, September, October.

Solar Time	21-Jun (MW)	21-Jul (MW)	21-Aug (MW)	21-Sep (MW)	21-Oct (MW)
5	2	0	0	0	0
6	67	53	20	0	0
7	144	131	98	51	7
8	216	204	175	129	76
9	277	267	241	197	144
10	324	315	292	250	197
11	354	345	323	283	231
12	364	355	334	295	242
13	354	345	323	283	230
14	324	315	291	250	197
15	277	267	241	197	144
16	216	204	175	128	76
17	144	131	98	50	6
18	67	53	19	0	0
19	2	0	0	0	0
20	0	0	0	0	0

Table 6b. Maximum estimate of PV power generation potential on San Francisco Rooftops during clear sky conditions calculated for the 21st of June, July, August, September, October.

Solar Time	21-Jun (MW)	21-Jul (MW)	21-Aug (MW)	21-Sep (MW)	21-Oct (MW)
5	5	0	0	0	0
6	166	132	49	0	0
7	356	324	243	125	17
8	533	504	432	318	189
9	685	659	595	488	357
10	801	777	720	618	487
11	874	852	799	700	570
12	899	877	826	728	598
13	874	852	799	700	569
14	801	777	720	617	487
15	685	659	595	487	356
16	533	504	431	317	187
17	356	323	242	123	16
18	166	131	48	0	0
19	5	0	0	0	0

Conclusions

The potential for rooftop PV power generation in San Francisco is large, both in terms of total output, and more importantly in terms of peak output, which corresponds well wit times of peak demand in San Francisco. Our low estimates for total output potential during peak times in late October (when potential is not at its highest) range from 240 MW to 600 MW, bounding the size of the proposed Potrero Unit 7, at 540 MW. Thus, even if only the low-end, conservative estimate of potential is achievable, peak output is not insignificant compared to Unit 7.

Acknowledgements

Karina Garbesi gratefully acknowledges support received from an Environmental Leadership Grant provided by the Switzer Foundation. The authors thank Denise Popolus for assistance in finding solar radiation data. The authors thank Robert Van Buskirk for providing data on power contract prices and PV system costs.

References

Ametek, I. 1984. *Solar Energy Handbook: Theory and Applications*. Chilton Book Company, Radnor, Pennsylvania.

CAISO (California Independent System Operator), City and County of San Francisco, Pacific Gas and Electric Company, and I. Stakeholders. 2000. San Francisco Peninsula Electric Transmission Long-Term Planning Technical Study.

Dames and Moore. 2000. Appendix A: Reliability Analysis. *Application for Certification for Potrero Power Plant Unit 7 Project: Volume II Technical Appendices*. Prepared for Southern Company (now Mirant).

Appendix A

Prices of Contracts for new Gas-fired Power Plant Capacity in California

Table A1 contains information derived from the business press on long-term contracts and memoranda of understanding for new capacity signed by Governor Davis. The range of prices for new capacity is between $4.6/W and $6.3/W.

	Price	Contract duration
Allegheny Energy Inc. 150 MW increase to 1000 MW over life of contract 10 years $4.6 billion Source: http://biz.yahoo.com/rf/010322/n22176051.html	$4.6/W	10 years
Duke Energy 550 MW 1/1/2002 increase to 800 MW 1/1/2003 9 years $4 billion Source: http://biz.yahoo.com/prnews/010305/chm021.html	$5.0/W	9 years
Calpine 200 MW 7/1/2001 increase to 1000 MW 1/2002 10 years $5.2 billion Source: http://biz.yahoo.com/prnews/010228/sfw087.html	$5.2/W	10 years
Calpine 90 MW 8/1/2001 increase to 495 MW 8/2002, 20 years $3.1 billion Source: http://biz.yahoo.com/prnews/010228/sfw087.html	$6.3/watt	20 years
Calpine 200 MW 10/2001 increase to 1000 MW 1/1/2004 10 years $4.6 billion Source: http://biz.yahoo.com/prnews/010228/sfw087.html	$4.6	10 years

Appendix B.

Estimating the Building Area Footprint of San Francisco

The building area footprint of San Francisco was determined using stratified random sampling of building area footprints included in a computerized map of the City (SF Micromap, CD-ROM by Zenrin). At about $40, the computerized map provided a least-cost approach to obtain building area footprint data. Moreover, its data were more current than databases available through the City of San Francisco's Planning Department, and far more convenient to use for our purposes. The map provides 2- and 3-dimensional representations of buildings as well as the locations of streets, parks, etc. The building images are based on a digitization of 1998 aerial photos supplemented by on-foot reconnaissance. Footprints of individual buildings can be measured on Micromap using a polygonal tool to outline the building.

Individual measurements of building area footprints using the polygon tool was too time consuming to obtain a sufficient number of samples for robust regional estimates. Therefore, we instead used a visual estimate of percent building coverage, and calibrated the visual estimates against paired samples in which all buildings were measured with the polygon tool. Fourty paired, randomly selected samples were used in the calibration. A linear regression of the visual data vs. the polygon-tool data was used to get the best estimate of percent building area (x_i) from each of the sampled visual estimates ($x_{i,v}$).

(C.1) $x_i = 6.13 + 0.906\, x_{i,v}$

Here the subscript, i, is used to indicate a generic individual sample. The results of the calibration analysis are shown in Figure C.1.

The standard error of the linear fit was calculated using S-Plus (statistics software), to obtain estimates of the errors anticipated over the range of building area percentages encountered. The resulting polynomial equation was used to calculate the uncertainty (aka error estimate, e) in individual sample estimates:

(C.2) $e_i = 4.79 – 0.1025\, x_{iv} + 0.0013 x_{iv}^2$

Together these yield building areas for individual samples known with 95% confidence to be $x_i \pm e_i$.

The City was divided into four regions that identify areas of roughly similar topography, land use, and or meteorology (see Table C1) . To increase sampling efficiency the sampling process eliminated largely undeveloped areas, specifically, the Presidio, the Legion of Honor, Golden Gate Park, and Lake Merced. These regions are described in Table 4.

When attempting to determine an average percentage from a random sub-sample of percentages, the binomial distribution determines the relationship between the needed sample size and the level of confidence obtained for the estimate of the population average in the following way,

C.4. $$n = p(1 - p)\left(\frac{z}{E}\right)^2$$

where, n is the number of samples needed, p is the fraction of land covered by buildings, z = 1.96 for a 95% confidence-level estimate, and E is the tolerable error in the estimate of p, also expressed as a fraction. In practice, p is 'guestimated' from a preliminary survey. Then the necessary n is found by setting the level of tolerance acceptable in the error, or adjusting the tolerable confidence level. Based on this approach, we sampled 140 data points per region. This allows us to combine data from any two regions to achieve reasonable errors at the 95% confidence level.

The percentage of land occupied by buildings in a given region is determined from the weighted arithmetic mean of the random-sample best estimates as follows:

$$X_r = \frac{\sum_{i=1}^{n} \frac{x_i}{e_i}}{\sum_{i=1}^{n} \frac{1}{e_i}} \quad . \qquad \text{(C.3)}$$

Appendix C:

Summary statistics of solar radiation at the San Francisco Airport

This appendix presents summary statistics from a 30-year solar radiation database for the San Francisco Airport. Statistics presented include the annual and 30-year maxima and averages of global solar radiation (direct plus diffuse) on a horizontal surface, statistics on the variability of those measures. The hourly meteorological data for the 30 year period were obtained form the National Renewable Energy Laboratory (NREL, a US Department of Energy Laboratory in Golden Colorado), which distributes 30-year records (1961 – 1990) of solar radiation online (http://rredc.nrel.gov/solar/old_data/nsrdb/hourly/).

This Solar and Meteorological Surface Observational Network (SAMSON) dataset is extracted from NREL's National Solar Radiation Database (NSRDB). The NSRDB solar radiation values for SF were not measured directly. Rather, they are calculated from theoretical clear-sky radiation and observed cloud cover recorded hourly at a meteorological monitoring station at the San Francisco Airport (Weather Bureau Army Navy Station #23234, N 37.62, W 122.38 at an elevation of 5 m). Global horizontal radiation (the combination of direct beam and diffuse radiation received on a horizontal surface at ground level) was used to represent the average sunlight incident on a horizontal PV panel (kWh/m^2/day).

The summary statistics presented in Table B1 below show that solar radiation is very stable in statistical terms even for a place with weather as variable as San Francisco's. Each line in the table presents particular values or averages taken from each year's hourly dataset. These include: the maximum global radiation measured during the year, the average annual radiation (in Wh/m^2 and in kWh/m^2/day), the average of the 365 highest radiation values in the year, and the 365th brightest value measured. The standard deviation is less than 2.5% of the average for all values recorded. Thus solar radiation is a reliable and predictable energy resource, even in a location with highly dynamic weather conditions, like San Francisco.

Table B1. Summary statistics from the 30-year SANSOM solar radiation database

Year	Maximum Global radiation (W/m^2)	Annual Average Wh/m^2	Annual average insolation kWh/m^2/day	Average 365 highest hours	365th most intense hour
1961	1014	196	4.71	926	857
1962	1016	198	4.74	934	869
1963	1032	190	4.56	931	856
1964	1008	196	4.70	916	851
1965	1014	191	4.58	932	862
1966	1015	196	4.71	936	867
1967	1013	194	4.65	928	854
1968	1020	193	4.63	927	858
1969	1019	199	4.77	933	869
1970	1018	203	4.88	933	872
1971	1011	203	4.88	933	865

1972	1022	198	4.75	936	865
1973	1021	198	4.76	937	877
1974	1022	197	4.74	937	874
1975	1031	199	4.78	934	870
1976	1027	196	4.71	921	846
1977	1011	194	4.66	912	840
1978	1023	196	4.70	930	855
1979	1025	196	4.70	931	857
1980	1012	196	4.70	911	839
1981	1020	200	4.80	929	869
1982	1003	190	4.56	915	846
1983	1003	184	4.41	917	847
1984	1015	203	4.87	932	872
1985	1017	199	4.77	920	848
1986	1007	197	4.73	922	851
1987	1024	194	4.65	907	841
1988	1008	201	4.83	924	853
1989	1016	198	4.76	931	868
1990	1015	203	4.86	944	853
Average	1017	197	4.72	927	858
Standard Deviation	7	4	0.10	9	11
Standard Deviation (% of Average)	0.72%	2.21%	2.21%	0.97%	1.27%